Computers, Environment and Urban Systems 97 (2022) 101866

Contents lists available at ScienceDirect

Computers, Environment and Urban Systems

journal homepage: www.elsevier.com/locate/ceus

Predicting the variability in pedestrian travel rates and times using crowdsourced GPS data

Michael J. Campbell [a,*], Philip E. Dennison [a], Matthew P. Thompson [b]

[a] Department of Geography, University of Utah, 260 S Central Campus Dr, Rm 4625, Salt Lake City, UT 84112, USA
[b] Rocky Mountain Research Station, USDA Forest Service, 240 W Prospect, Fort Collins, CO 80526, USA

ARTICLE INFO

Keywords:
GIS
GPS
Pedestrian
Travel rate
Travel time
Least-cost path

ABSTRACT

Accurately predicting pedestrian travel times is critically valuable in emergency response, wildland firefighting, disaster management, law enforcement, and urban planning. However, the relationship between pedestrian movement and landscape conditions is highly variable between individuals, making it difficult to estimate how long it will take broad populations to get from one location to another on foot. Although functions exist for predicting travel rates, they typically oversimplify the inherent variability of pedestrian travel by assuming the effects of landscapes on movement are universal. In this study, we present an approach for predicting the variability in pedestrian travel rates and times using a large, crowdsourced database of GPS tracks. Acquired from the outdoor recreation website AllTrails, these tracks represent nearly 2000 hikes on a diverse range of trails in Utah and California, USA. We model travel rates as a function of the slope of the terrain by generating a series of non-linear percentile models from the 2.5 th to the 97.5 th by 2.5 percentiles. The 50 th percentile model, representing the hiking speed of the typical individual, demonstrates marked improvement over existing slope-travel rate functions when compared to an independent test dataset. Our results demonstrate novel capacity to estimate travel time variability, with modeled percentiles being able to predict actual percentiles with less than 10% error. Travel rate functions can also be applied to least cost path analysis to provide variability in travel times.

1. Introduction

Pedestrian travel times, or the time it takes individuals to travel on foot between locations, are used across a diverse array of professional and academic disciplines (Rout, Nitoslawski, Ladle, & Galpern, 2021). Urban planners use travel time to assess walkability, access to critical resources, such as grocery stores and medical facilities, and even as a predictor of neighborhood-level income inequality (dos Anjos Luis & Cabral, 2016; Ewing & Handy, 2009; Reyes, Páez, & Morency, 2014; Widener et al., 2017; Yang et al., 2015). Recreation management professionals can incorporate travel time predictions into the strategic development of new hiking trails and improved understanding of trail use and recreation preferences (Chiou, Tsai, & Leung, 2010; Márquez-Pérez, Vallejo-Villalta, & Álvarez-Francoso, 2017; Meijles, de Bakker, Groote, & Barske, 2014; Orsi & Geneletti, 2016; Xiang, 1996). Travel time is an important component of remoteness, which is important for mapping and assessing wilderness quality and recreation suitability (Carver, Comber, McMorran, & Nutter, 2012; Kliskey, 2000). To ensure their safety, wildland firefighters need to know how long it will take them to retreat to a safety zone or other low-risk area in dangerous situations (Beighley, 1995; Campbell, Page, Dennison, & Butler, 2019; Sullivan, Campbell, Dennison, Brewer, & Butler, 2020). Search and rescue teams need to know how long it will take them to reach an injured hiker to ensure that they can effectively plan their rescue operation (Ciesa, Grigolato, & Cavalli, 2014). Emergency response planners use travel times to simulate evacuations in the event of tsunamis, earthquakes, or other natural disasters (Bernardini, Santarelli, Quagliarini, & D'Orazio, 2017; Wood & Schmidtlein, 2012). Police need to establish search perimeters for missing persons, knowing how far they may have traveled in a given period of time (Doherty, Guo, Doke, & Ferguson, 2014; Shalev, Schaefer, & Morgan, 2009). Military personnel can benefit from accurate pedestrian travel time estimation in many ways, including a basic understanding of how long it will take ground troops to reach a target location (Fields, 1995).

* Corresponding author at: 260 S Central Campus Dr, Rm 4625, Salt Lake City, UT 84112, USA.
E-mail addresses: mickey.campbell@geog.utah.edu (M.J. Campbell), dennison@geog.utah.edu (P.E. Dennison), matthew.p.thompson@usda.gov (M.P. Thompson).

https://doi.org/10.1016/j.compenvurbsys.2022.101866
Received 4 June 2022; Received in revised form 27 July 2022; Accepted 30 July 2022
Available online 20 August 2022
0198-9715/

The prediction of travel times is inexorably linked with the prediction of travel rates. However, the rate of pedestrian travel is highly variable among human populations. This variability is partially dictated by intrinsic factors, such as one's degree of energy expenditure, level of fitness, and physiological characteristics (Gottschall & Kram, 2003; Minetti, Moia, Roi, Susta, & Ferretti, 2002; Wu & Zhao, 2021). It is also partially dictated by extrinsic factors, such as terrain slope, the ground surface condition, and obstructing landscape features (Campbell, Dennison, & Butler, 2017; Pandolf, Givoni, & Goldman, 1977; Peterson, Brownlee, & Marion, 2018; Tobler, 1993; Wolf & Wohlfart, 2014). The relationship between these intrinsic and extrinsic factors is perhaps one of the most fundamental human-environment interactions – one that not only defines the instantaneous speed of pedestrian movement, but also the time it takes to travel between locations, and the selection of optimal routes that minimize time, effort, or both (Campbell, Dennison, Butler, & Page, 2019; Márquez-Pérez et al., 2017; White, 2015). Travel time variability and uncertainty has been studied extensively in the context of non-pedestrian modes of travel, such as driving and taking public transit, with a particular focus on urban areas (e.g., Chen et al., 2017; Chen, Wang, Wang, & Lam, 2019; de Palma & Picard, 2005; Ettema & Timmermans, 2006). However, research into the prediction of pedestrian travel time variability is limited. What evidence there is comes primarily from studies of tsunami evacuation (C. Chen, Mostafizi, Wang, Cox, & Cramer, 2022; Fraser et al., 2014). C. Chen et al. (2022) compiled GPS-tracked travel rates from an evacuation drill, modeling a probability distribution function of travel rates, though their analysis of the relationship between slope and travel rates resulted in a singular predictive function that does not account for variability in travel rate. There remains a critical need for a broadly-applicable set of predictive functions for pedestrian travel time variability under a diverse range of terrain conditions.

There are two broad approaches to quantifying pedestrian travel rate variability: (1) at the individual level; and (2) at the population level. At the individual level, it is theoretically possible to derive a function that accounts for all of the intrinsic factors and extrinsic factors that determine travel rate, as well as the interactions between those factors. Applied physiology research has made strides towards that end (Looney et al., 2019; Ludlow & Weyand, 2017; Minetti et al., 2002; Pandolf et al., 1977; Santee, Blanchard, Speckman, Gonzalez, & Wallace, 2003). By incorporating variables such as body mass, oxygen consumption rates, and external load carriage, and how they interact with the terrain slope and surface type, these studies have the potential to quantify variability at the scale of the individual; however, travel rate is not the prediction of interest in these studies. Instead, the focus is on metabolic cost of movement, where travel rate is a variable. Though it is possible to solve these equations for travel rate (e.g., Herzog, 2010), doing so requires a precise understanding of an individual's or a group of individuals' quantitative energy expenditure. As a result, their capacity for estimating travel time variability among broad populations is limited.

Given this limitation, studies that quantify variability at the population level tend to ignore the intrinsic factors and focus on how various landscape conditions such as slope, ground surface conditions, and vegetation affect movement (Campbell et al., 2017; Campbell, Dennison, et al., 2019; Davey, Hayes, & Norman, 1994; Higgins, 2021; Irmischer & Clarke, 2018; Kay, 2012; Márquez-Pérez et al., 2017; Naismith, 1892; Rees, 2004; Tobler, 1993). However, the fundamental limiting assumption in most of these studies is that the effects of landscape conditions on travel rates will be consistent from one individual to another. These efforts date back to the late 19th century, with Naismith's Rule predicting one hour of travel time for every three miles (4.8 km) of horizontal distance, and an additional hour for every 2000 ft. (609.6 m) of vertical distance (Carver et al., 2012). The most popular of these is Tobler's Hiking Function (Goodchild, 2020; Tobler, 1993) which, like Naismith's Rule, uses the slope of the terrain as the basis of travel rate prediction. This function does incorporate one dimension of variability by adding a multiplier to adjust for on-trail versus off-trail travel, though it assumes that all individuals on- and off-trails travel at the same rate. Likewise, Davey et al. (1994) allows for modification based on an individualized flat-slope travel rate, but does not provide likely bounds for estimating variability across a large number of individuals (Davey et al., 1994). Irmischer and Clarke (2018) produced four slope-travel rate predictive functions, broken down by sex (male versus female) and route type (on-trail versus off-trail), but the variability within these four categories remains high (Irmischer & Clarke, 2018).

Campbell, Dennison, et al. (2019) sought to address the question of travel rate variability using a large database of crowdsourced GPS-derived travel rate data. Using a percentile modeling approach, they produced a series of functions that predicted travel rate based on slope from very slow to very fast movement. Although an important step towards quantifying travel rate variability, this study had some critical limitations. The data used made no distinction between walking and running. Thus, their results cannot be applied to the travel mode-specific prediction of rates. The data were aggregated to relatively short trail segments, rather than entire trails, which limited the capacity for estimating travel time for continuous hiking over longer distances, as one can travel at unsustainably-fast rates over short distances. Travel rate data did not have any individually-identifying information – only anonymized travel rates for each trail segment. This meant that there was no way to link together travel rate records to determine if a record was part of a short or long hike, and no way to differentiate individual-level slope-travel rate relationships along entire hikes. Lastly, the data came from a fitness tracker social media app that is focused on travel rate comparison, introducing an element of competition that likely resulted in an upward bias of travel rates.

The goal of this research is to quantify and enable the prediction of pedestrian travel time variability among a broad population. To do this, we use a large, crowdsourced database of raw GPS track data, gathered from AllTrails (https://www.alltrails.com/), an outdoor recreation website and mobile app. By comparing thousands of GPS tracks to landscape slope derived from high-resolution, airborne lidar data, we gain novel insight into the slope-travel rate variability. And by quantifying the range of slope-predicted travel rates among this population, we produce a series of equations that enable the prediction of independently-validated travel time ranges. The results of this study can be applied in the broad range of contexts within which travel time prediction is of importance.

2. Methods

2.1. Data and study areas

To enable the creation of broadly-representative predictive travel rate functions, we gathered GPS track data from a large number of individuals ($N = 1955$) on 20 trails, evenly split between trails near Salt Lake City, Utah, USA and Los Angeles, California, USA (Table A1, Appendix A). These cities were selected because they both feature high population densities in close proximity to abundant hiking trails, a diverse range of terrain conditions, and freely-available airborne lidar data for comparing GPS data to precise terrain data. For each city, the 10 most popular trails as defined by AllTrails were selected for this study. All publicly-available, high-quality, hiking season data from 2021 were downloaded. Track quality was qualitatively visually interpreted individually for each track. A track would not be downloaded if it met any of the following criteria: (1) poor GPS signal, as evident by a track line that consistently deviated more than 10 m from the mapped trail; (2) too short (track was less than approximately one quarter of the mapped trail's length); (3) too long (track extended well beyond mapped trail and followed along other trails or roads for a distance greater than approximately one tenth of the mapped trail's length); (4) any activity other than "hiking" indicated (e.g., "running", "mountain biking", etc.). Hiking season was defined as May through September for Salt Lake City and April through November for Los Angeles, given the likely presence of snow or higher probability of inclement weather in the mountains before and after those temporal windows.

2.2. Trail creation and snapping

GPS units have inherent position uncertainty owing to a variety of factors including the number and geometry of satellites providing positional information, both of which contribute to dilution of precision (Rustamov & Hashimov, 2018; Santerre, Geiger, & Banville, 2017). This is particularly true of the types of GPS receivers that are commonly used for recreational activities, such as tracking hikes (Korpilo, Virtanen, & Lehvävirta, 2017; Meijles et al., 2014). Although the GPS data we downloaded from AllTrails did not provide accuracy or device information, we assume that most GPS tracks were collected using smartphones and smartwatches. The accuracy of these devices varies greatly by manufacturer, model, age, and environmental conditions, ranging anywhere from submeter to more than 20 m (Merry & Bettinger, 2019). Given the fact that the trails in this study tend to be located in mountainous areas, positional error of even a few meters can significantly limit the ability to accurately compare GPS points to spatially-coincident lidar data, which is essential for deriving accurate terrain slope information. To resolve this limitation, we developed a procedure to "snap" GPS points to the nearest location along the trail. This requires a positionally-accurate linear geospatial feature that represents each trail. After a preliminary review of existing trails GIS data revealed persistent inaccuracy and/or imprecision, we opted to create our own trails data, using the procedure outlined in Fig. 1. This procedure begins by compiling all of the GPS tracks for each trail of interest (Fig. 1A). It then generates a kernel density raster, representing the spatial concentration of those GPS points (Fig. 1B). We assume that the "true" trail location can be captured by the locations of highest GPS point density. Accordingly, the algorithm then adjusts the linear trail feature acquired from AllTrails to align with the raster cells of highest point density (Fig. 1B). Lastly, each point in each GPS track is then snapped to the nearest point along the newly-generated trail (Fig. 1C).

2.3. Travel rate and slope calculation

For each GPS track, horizontal (two-dimensional) distance was calculated as the distance between successive points in x and y directions. Travel rates were calculated as the horizontal distance between successive points divided by the GPS time between the same points. To ensure a maximally-precise comparison between travel rates and spatially-coincident terrain slope, we extracted ground elevations from 1 m-spatial resolution, airborne lidar-derived digital terrain models, acquired from the United States Geological Survey 3D Elevation Program (Sugarbaker et al., 2017).

2.4. GPS data filtering

Filtering the GPS points was necessary to eliminate noisy or erroneous data. All points that had a snapping distance (distance between original GPS point and trail-snapped point locations) greater than 10 m were removed. We assume these points to be either inaccurate GPS points, or a detour was taken from the trail of interest. All points with a GPS collection interval of less than 3 s or greater than 30 s were also removed. Preliminary analysis revealed that high-frequency points (1 s, 2 s intervals) produced very noisy travel rate estimates. Low-frequency points failed to precisely capture the relationship between local-scale terrain and travel rates. All points with travel rates less than 0.2 ms^{-1} were removed, as these points represent likely stoppage time (e.g., taking breaks while on an ascent, or at a viewpoint) plus drift of GPS coordinates. This 0.2 ms^{-1} threshold was chosen by examining histograms of the travel rate data, where we found an uptick in data frequency at and below this threshold, which we attributed to GPS points that would result from extended periods of stoppage. All points with travel rates greater than 5 ms^{-1} were removed since these speeds indicate running, and points with terrain slopes of less than -30° or greater than 30° were removed, as they were poorly represented in the dataset and could possess outsized leverage on the modeling process. Finally, all points greater than or less than two standard deviations of the mean travel rate within a two-minute moving window were removed, as these may represent either erroneous or unrepresentative sudden increases or decreases in speed. This filtration process removed approximately 23% of the GPS points (Table A1, Appendix A).

2.5. Slope-travel rate smoothing

As discussed in the Introduction, instantaneous travel rates are highly variable, even at a given terrain slope, both between individuals, but also within an individual's hike. In this study, we are interested primarily in the "between individuals" variability. Variability within an individual's hike can stem from a variety of sources, including varied exertion levels (e.g., moving faster at the start of a hike than at the end) and trail traffic (e.g., moving slower while hiking behind a group). To remove this within-hike variability, we performed a slope-travel rate smoothing process, calculating the median travel rate using a moving window of one degree of slope. An example of this can be seen in Fig. 2. The resulting travel rates are thought to be a more accurate

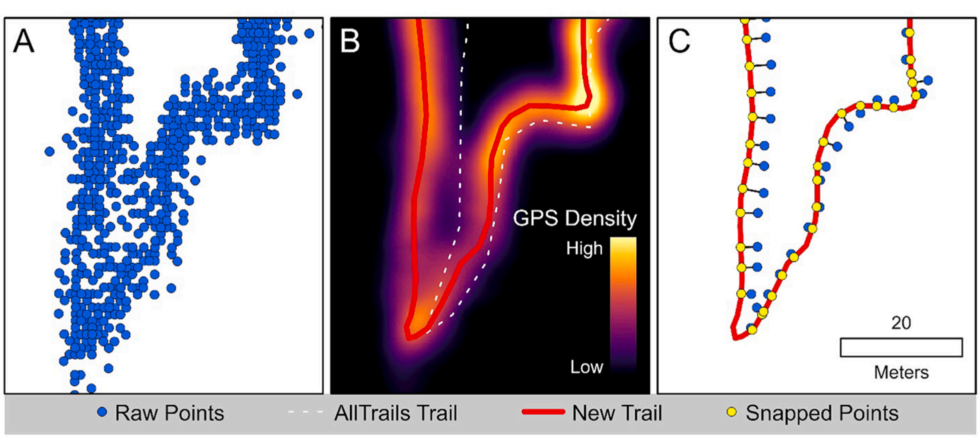

Fig. 1. Example of trail delineation and GPS point snapping procedure. Raw GPS points (A) are used to derive a kernel density raster that drives the spatial adjustment of the original trail line from AllTrails to a new trail line based on maximum GPS point density (B). This new trail is then used to snap each raw GPS point to the closest point along the new trail (C).

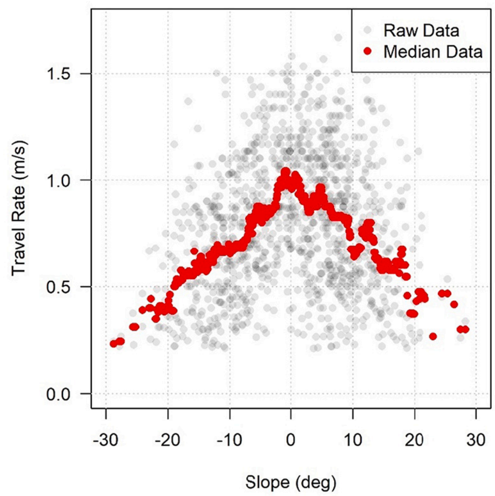

Fig. 2. Example of the slope-travel rate smoothing process for a single GPS track, whereby median travel rates within a moving window of one degree of slope are calculated from the raw GPS-derived slope-travel rate data.

representation of the "hike-level" relationship between slope and travel rate.

2.6. Slope-travel rate percentile modeling

All of the slope-travel rate smoothed tracks were compiled, and then split at random into training data (80% of tracks) and test data (20% of tracks). Using the training data, non-linear quantile regression was used to generate a series of models from the 2.5th percentile to the 97.5th percentile by 2.5 percentile interval (39 models in total). A modified Lorentz function form was used (Campbell, Dennison, et al., 2019; Sullivan et al., 2020):

$$r = c\left(\frac{1}{\pi b\left(1+\left(\frac{s-a}{b}\right)^2\right)}\right) + d + es \tag{1}$$

where r is the travel rate in ms^{-1}, s is the slope in degrees, and a, b, c, d, and e are model coefficients. For a detailed review of the role that each of these coefficients play in predicting travel rates, please refer to (Campbell, Dennison, et al., 2019). Although the primary focus for our analysis is travel rate variability, and thus each percentile model is important, we also recognize that there is value in having a singular function that is most representative of the typical pedestrian's speed. In the context of percentile modeling, this would be the 50th percentile, or the median model. We assessed the accuracy of this model using the travel rates from the 20% test data previously set aside. To compare the extent to which this new function improves upon popular existing slope-travel rate predictive functions, we also assessed the accuracy of the following models: Tobler's hiking function for on-trail movement (Tobler, 1993), the function from Rees (2004), the modified Tobler's hiking function from Márquez-Pérez et al. (2017), male-female averaged functions for both on-trail and off-trail travel from Irmischer and Clarke (2018), the 5th percentile slope-travel rate model from Campbell, Dennison, et al. (2019), and the "low" and "moderate" speed functions from Sullivan et al. (2020). All of the above were assessed using two error metrics, root mean squared error (RMSE) and bias, as follows:

$$RMSE = \sqrt{\frac{\sum_{i=1}^{n}(\hat{y}_i - y_i)^2}{n}} \tag{2}$$

$$bias = \frac{\sum_{i=1}^{n}(\hat{y}_i - y_i)}{n} \tag{3}$$

where $\hat{y}_i$ is the predicted travel rate for point i and y_i is the actual travel rate for point i for all points $[i\ldots n]$. Calculating RMSE and bias for the entire dataset provides insight into overall performance across all slopes tested, but fails to capture the nuance of model performance at different slopes. For example, a model that significantly underestimates travel rates on steep slopes but overestimates travel rates on flat slopes could result in a bias of 0 ms^{-1}, giving the false appearance of model accuracy. Accordingly, RMSE and bias were also calculated per degree of slope to assess these nuanced effects.

2.7. Travel time accuracy assessment

The travel rate accuracy assessment described above provided valuable insight into the performance of the singular, median model, but did not provide a sense for how well the percentile models can predict travel time variability. To that end, we acquired additional GPS track data for three popular trails outside of the study regions to test the broad applicability of the models (Table A2, Appendix A). They were selected based on popularity, diversity in length (one short, one medium, one long), and diversity in geography (Northeast, Southeast, and Northwest US).

The trails were delineated and tracks were snapped to the trail, in the exact same manner as described in Section 2.2. Travel rates and times were then computed for each GPS point, using the same procedure described in Section 2.3. Points greater than 30 m from the trail were removed, as were points with travel rates less than 0.2 ms^{-1}. We used a 30 m threshold rather than the 10 m threshold used previously to retain as much GPS data as possible, accommodating low GPS accuracy and ensuring total travel time accuracy. Total travel times were computed as the sum of elapsed times between each remaining GPS point.

To compare these actual travel times with modeled travel times, we used each of the travel rate percentile models (2.5th to 97.5th, by 2.5 percentiles) to predict total travel time for each of the three trails. To do this, we generated points every 2 m along the trail, calculated the slope between each sequential point, and estimated the time it would take to travel between points at each travel rate percentile. For each trail, these travel times were summed to produce 39 total travel time estimates, one for each modeled percentile. These modeled values were compared to percentiles of the actual total travel times, and RMSE and bias were calculated for each trail individually as well as for all three trails combined. Relative RMSE (rRMSE) and bias (rbias) were also calculated by dividing each error metric by the mean of the true values, as they provide an easily-interpretable measure of proportional error, calculated as follows:

$$rRMSE = \frac{\sqrt{\frac{\sum_{i=1}^{n}(\hat{y}_i - y_i)^2}{n}}}{\frac{\sum_{i=1}^{n} y_i}{n}} \tag{4}$$

$$rbias = \frac{\frac{\sum_{i=1}^{n}(\hat{y}_i - y_i)}{n}}{\frac{\sum_{i=1}^{n} y_i}{n}} \tag{5}$$

To determine the extent to which the singular, median travel rate model demonstrates improvement over other singular slope-travel rate predictive models, the median travel time for each of the three test trails was compared to modeled travel times for each predictive model outlined in Section 2.6.

2.8. Demonstration of application

To demonstrate the utility of our travel time variability prediction approach, we present a theoretical use case using least-cost path modeling. Least-cost path modeling is a popular geospatial analysis technique for determining the path of least resistance between an origin and a destination (Adriaensen et al., 2003; Douglas, 1994; Goodchild, 1977). In the context of human pedestrian movement, the slope of the terrain is the most common impediment used to determine optimal routes and associated travel rates and times (Herzog, 2014). It is important to note that other landscape conditions, such as the presence, abundance, and arrangement of vegetation can have a significant impact on route selection and travel time; however, there is only limited evidence to date to accurately quantify these effects (Campbell et al., 2017). Accordingly, our new models can not only predict the optimal route that minimizes slope-based travel time, but also estimate the range and distribution of times it would take for a broad population of individuals to get from origin to destination. To demonstrate this, we used a 10 m-resolution digital elevation model from the Wasatch Mountains outside of Salt Lake City, UT with randomly-generated origin and destination points. We used the 50th percentile model to map the least-cost path between origin and destination. We extracted elevations from every raster cell along the least-cost path and predicted accumulated travel time between cells for each of the percentile models.

3. Results

3.1. Slope-travel rate smoothing

In total, the data in this study came from 1999 GPS tracks, containing over four million GPS points on trails ranging in hike length from approximately 2.8 km to 17.9 km. The distribution of slope-travel rate data used to train and test the travel rate percentile models can be seen in Fig. 3. Fig. 3A represents the instantaneous travel rate data, whereas Fig. 3B represents the slope-smoothed travel rate data. Both datasets demonstrate the typical relationship between slope and travel rate – that is, people tend to move faster on flatter slopes and slower on steeper slopes, both uphill and downhill. The slope-smoothed data possess a much narrower range of travel rates, as expected, given that within-hike variability is removed. The remainder of the results will be focused on the slope-smoothed travel rate data as these will be used for prediction of travel rates and times and the variability therein.

3.2. Slope-travel rate percentile modeling

The percentile model coefficients can be seen in Table A3, Appendix A. The values for coefficients a, b, c, d, and e can be fed into Eq. 1 to predict travel rates at a given slope and percentile. For example, if one wanted to predict the range of travel rates representative of 95% of the population, one could use the 2.5th percentile and 97.5th percentile coefficients.

Fig. 4 illustrates a comparison between true percentiles calculated from slope-smoothed travel rate training data, binned by degree of slope (Fig. 4A) and the modeled percentiles (Fig. 4B). The models accurately capture the shape of the true percentiles with some minor deviations on steeper slopes and higher percentiles, where the models tend to underestimate travel rates. However, given the sparseness of data at extreme slopes, the uptick in travel rates at extreme slopes in the true percentiles is likely the result of noise, as it is unlikely that people move significantly faster at 30° uphill than they do at 28°. In addition, the true percentiles tend to produce a "shelf" of consistent travel rates between approximately −7° and 3° of slope, whereas the functional form of the Lorentz curve (Eq. 1) tends to produce a more rounded curve peak. As a result, travel rates on near flat slopes at likely slightly overestimated, whereas on slight uphill and downhill slopes they are likely slightly underestimated. Alternative functions were tested to try to accommodate the shape of the shelf, but did not improve fit over Eq. 1. As discussed in Section 2.6, although the focus of this study is on travel rate variability, it is still useful to have a singular predictive function in many situations. The 50th percentile function, which represents the average pedestrian hiking rate based on slope, is highlighted in red (Fig. 4).

A comparison between the 50th percentile function and an array of popular, existing slope-travel rate functions reveals general agreement (Fig. 5). Most functions reach a peak travel rate at a slightly downhill slope with steadily decreasing travel rates as slope increases or decreases on either side of the peak. The 50th percentile function reaches a maximum travel rate of 1.15 ms^{-1} at a slightly downhill slope of −1.53°. A key difference among these function is the shape of the curve peaks, with Tobler (1993) and Márquez-Pérez et al. (2017) coming to a pronounced peak, in what is known as a double-exponential or Laplace function form, whereas the other models (including our new model) feature a more rounded peak. Previous research has shown that the sharp peak results in overestimation of maximum travel rates (Campbell, Dennison, et al., 2019).

When comparing these functions to the travel rate test dataset, the new function outperforms others in terms of both overall error, as captured by RMSE (Fig. 6A), and the propensity for over- or

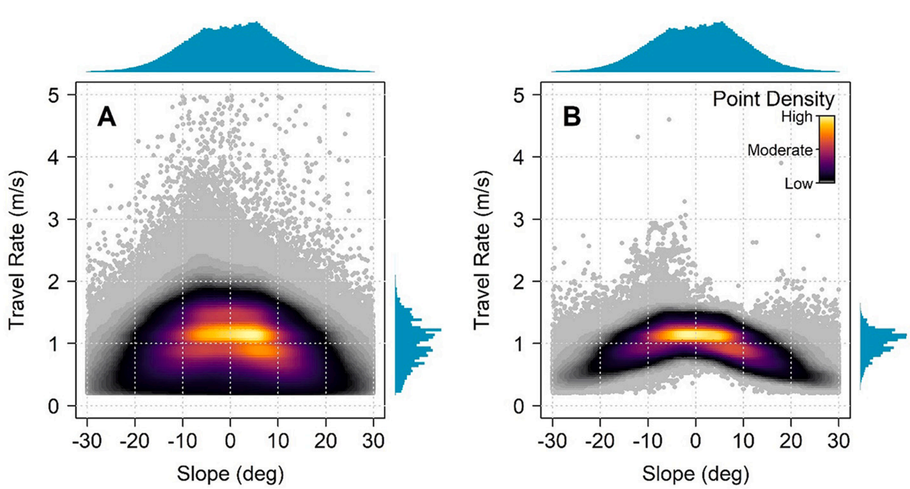

Fig. 3. Distribution of all GPS-derived slope-travel data, including both training and test data, used in the percentile-based travel rate modeling procedure, including the instantaneous travel rate data (A), as well as the slope-smoothed travel rate data (B).

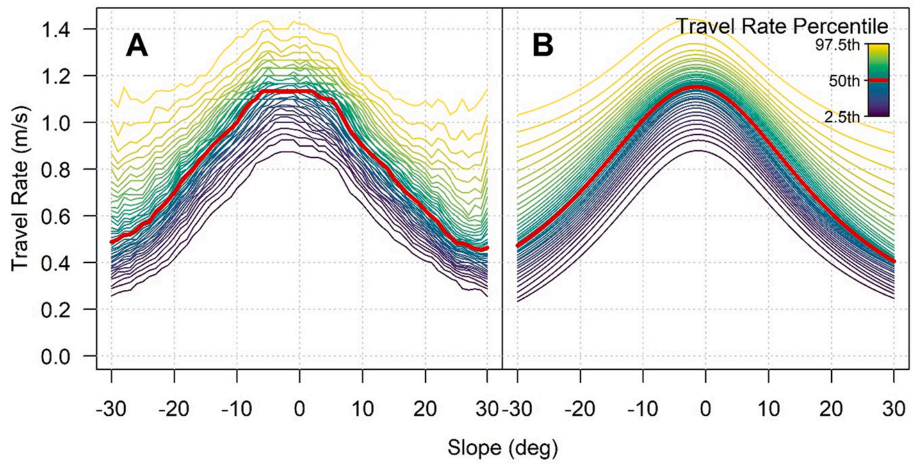

Fig. 4. Comparison between true percentiles calculate from slope-smoothed travel rate training data, binned by degree of slope (A) and the modeled percentiles (B).

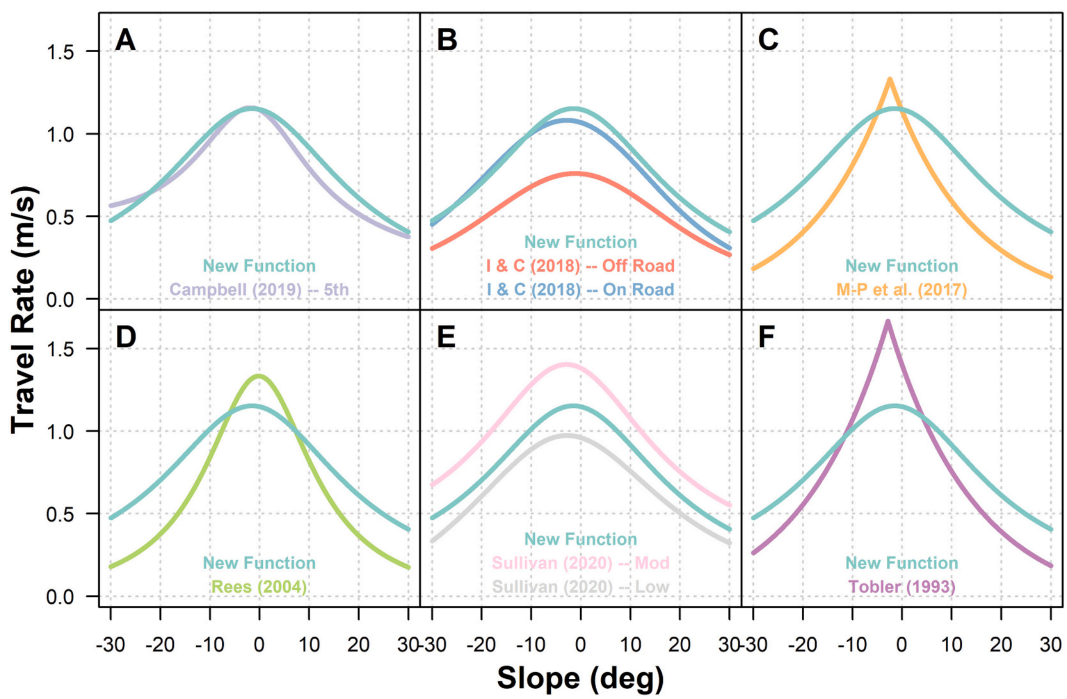

Fig. 5. Comparison between the new function (50th percentile function) and a range of popular, existing functions for predicting pedestrian travel rate based on terrain slope, including (A) Campbell, Dennison, et al. (2019)'s 5th percentile function, (B) Irmischer and Clarke (2018)'s on- and off-road functions, (C) Márquez-Pérez et al. (2017)'s function, (D) Rees (2004)'s function, (E) Sullivan et al. (2020)'s low and moderate functions, and (F) Tobler (1993)'s function-.

underestimating travel rates, as captured by bias (Fig. 6B). However, integrating the accuracy assessment results across the full range of slopes does not tell the full story, given the high concentration of data on lower slopes and the lower concentration of data on steeper slopes. Figs. 7 and 8 provide accounts of the performance of these functions by degree of slope. Once again, the new function tends to outperform the others across most slopes, with RMSE being consistently among the lowest (Fig. 7), and bias being consistently nearest to zero (Fig. 8). Nearly all of the models tend to perform better on flatter slopes – perhaps due to greater abundance of data in these conditions – with the exception of Tobler's Hiking Function, whose peaked nature results in significant overestimation of peak travel rates (Campbell, Dennison, et al., 2019; Higgins, 2021; Márquez-Pérez et al., 2017).

3.3. Travel time accuracy assessment

The results of the travel time variability accuracy assessment can be seen in Fig. 9 and Table 1. Comparing modeled to actual travel time percentiles on the three test trails yields results that fall near the 1:1 line, suggesting general agreement between the two (Fig. 9). Across all three trails, travel time percentiles were estimated within 0.26 h, or 15.6 min on average, which represents an error of approximately ±9% of the true travel time (Table 1). Bias is nearly zero across the three trails, suggesting that, on average, travel times are neither over- nor underestimated. A closer, trail-level examination, however, reveals some more nuanced errors. The longest trail, Alum Cave Trail to Mount Leconte, produced the highest absolute RMSE, but this is partly due to the trail length which produced the longest modeled and actual travel times, as evident by the moderate rRMSE value. Conversely, the shortest trail, Mount Willard Trail, produced the lowest absolute RMSE, but had the

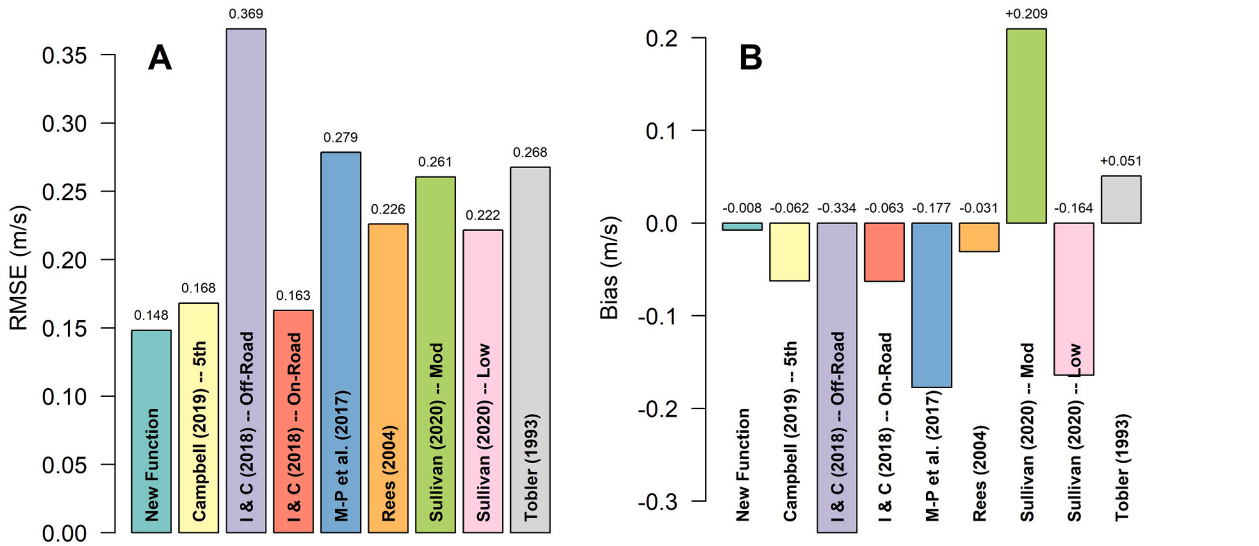

Fig. 6. Travel rate accuracy assessment results comparing new 50th percentile function to other popular slope-travel rate predictive functions, including RMSE (A) and bias (B), integrated across all slopes.

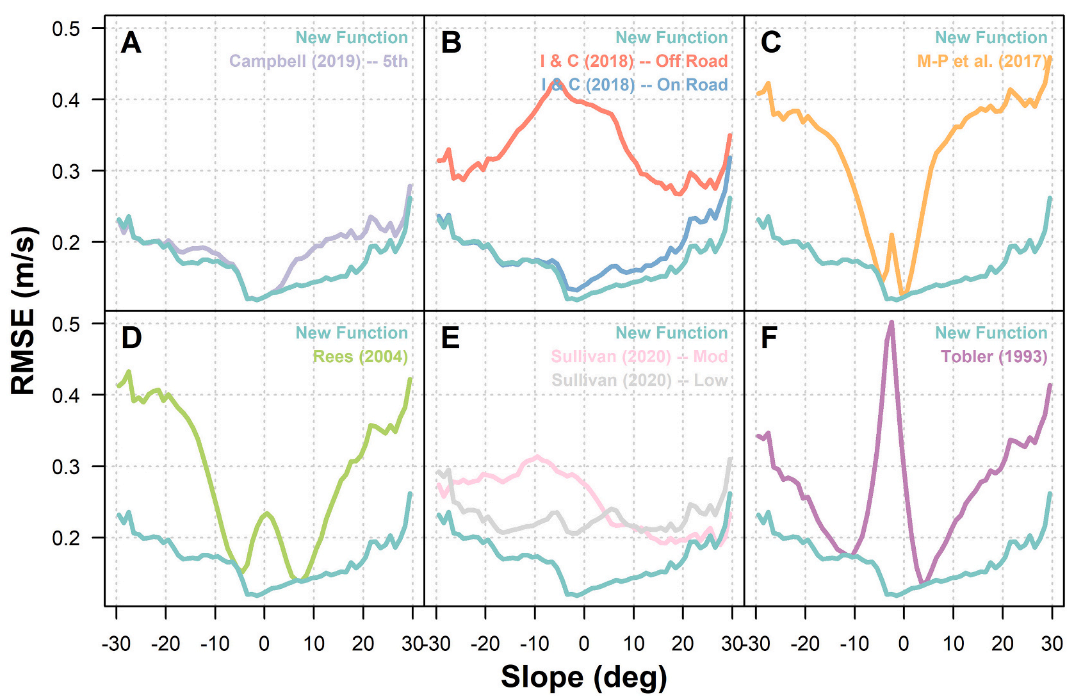

Fig. 7. Travel rate accuracy assessment results comparing new 50th percentile function to other popular slope-travel rate predictive functions, including (A) Campbell, Dennison, et al. (2019)'s 5th percentile function, (B) Irmischer and Clarke (2018)'s on- and off-road functions, (C) Márquez-Pérez et al. (2017)'s function, (D) Rees (2004)'s function, (E) Sullivan et al. (2020)'s low and moderate functions, and (F) Tobler (1993)'s function, calculated using root mean squared error by degree of slope.

highest rRMSE. Overall, the shortest trail (Willard) tended to result in underestimation of travel times (negative bias) and the longest trail (Alum) tended to result in overestimation of travel times (positive bias), whereas the mid-length trail (Skyline) resulted in the highest prediction accuracy, both in rRMSE and rbias. This may be due to the fact that the trails used to train the model had an average length that is identical to the length of Skyline Trail Loop (8198 m). In addition, the higher percentiles (faster movement) tended to underestimate travel time, whereas the lower percentiles (slower movement) tended to overestimate travel time.

The results comparing the singular, median travel rate predictive model with other singular slope-travel rate functions can be seen in Table 2. As described above, the new function tends to underestimate travel times on the two shorter trails (Skyline Trail Loop and Mount Willard Trail) and overestimate on the longer trail (Alum Cave Trail). However, averaging out the bias across all three trails, the new median function has the lowest absolute bias, underestimating travel time by approximately 2 min. The next best-performing model (that of Campbell, Dennison, et al., 2019) has a positive bias of nearly 9 min. Irmischer and Clarke (2018)'s on-road model is the third best, with an average overestimation of 10 min. Notably, Tobler's hiking function – certainly the most widely-used among these functions – has an average bias of

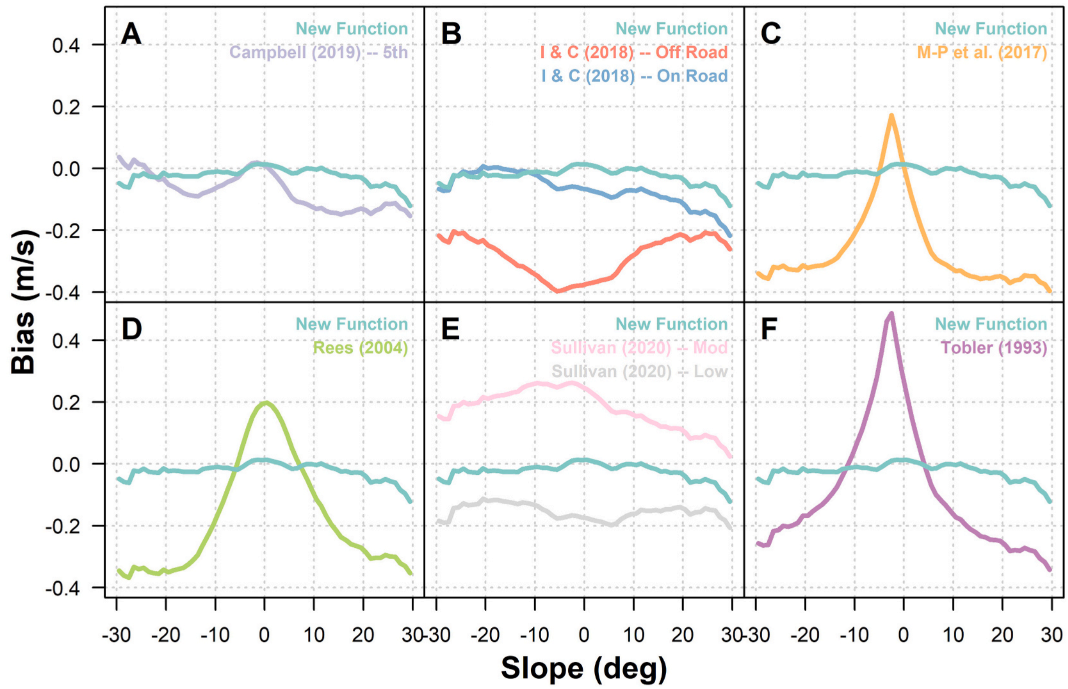

Fig. 8. Travel rate accuracy assessment results comparing new 50th percentile function to other popular slope-travel rate predictive functions, including (A) Campbell, Dennison, et al. (2019)'s 5th percentile function, (B) Irmischer and Clarke (2018)'s on- and off-road functions, (C) Márquez-Pérez et al. (2017)'s function, (D) Rees (2004)'s function, (E) Sullivan et al. (2020)'s low and moderate functions, and (F) Tobler (1993)'s function, calculated using bias by degree of slope.

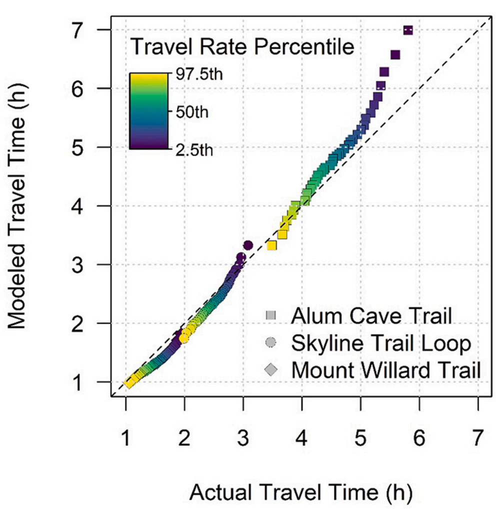

Fig. 9. Graphical travel time variability accuracy assessment results, comparing modeled travel time percentiles to actual travel time percentiles on three different hiking trails.

Table 1
Quantitative travel time variability accuracy assessment results.

Trail	RMSE (h)	rRMSE (%)	bias (h)	rbias (%)
Alum Cave Trail to Mount Leconte	0.39	8.58	0.28	6.13
Skyline Trail Loop	0.15	5.91	−0.11	−4.44
Mount Willard Trail	0.18	11.72	−0.17	−11.29
All	**0.26**	**9.17**	**0.00**	**−0.03**

Table 2
Comparison of modeled travel times on three test trails generated using the new, median travel rate predictive function and a host of existing travel rate functions. Numbers represent estimation bias in minutes from the actual median travel rates among the GPS-recorded travel times for each trail (Alum Cave Trail = 271.12 min; Skyline Loop Trail = 149.98 min; Mount Willard Trail = 89.82 min). The last column represents a mean bias for all three trails.

Travel Rate Model	Alum Cave Trail	Skyline Loop Trail	Mount Willard Trail	Mean for All Trails
New Function – Median	13.94	−8.49	−11.25	**−1.93**
Campbell, Dennison, et al. (2019) – 5th	29.52	2.23	−5.94	**8.60**
Irmischer and Clarke (2018) – Off-Road	151.91	58.64	26.42	**78.99**
Irmischer and Clarke (2018) – On-Road	37.15	0.16	−6.47	**10.28**
Márquez-Pérez et al. (2017)	206.40	47.62	13.75	**89.26**
Rees (2004)	117.09	17.10	−2.80	**43.80**
Sullivan et al. (2020) – Mod	−42.10	−34.45	−25.30	**−33.95**
Sullivan et al. (2020) – Low	81.05	18.20	3.49	**34.24**
Tobler (1993)	86.10	2.10	−9.42	**26.26**

over 26 min.

3.4. Demonstration of application

The modeled least-cost path between two randomly-selected origin and destination points in the Wasatch Mountains can be seen in Fig. 10. The route begins on fairly flat slopes and, as such, the resulting route is relatively straight. When a steep hill is encountered, the route takes a

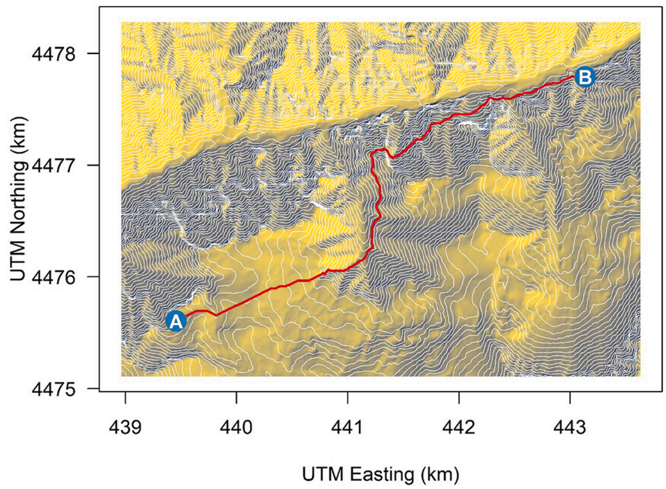

Fig. 10. Example least-cost path generated from predicting the fastest route from location A to location B in the Wasatch Mountains, based on the 50th percentile travel rate percentile model. Contour interval is 20 m and the terrain model is being displayed with a hillshade with a solar elevation of 45° and a solar angle of 135°.

sharp northerly turn and follows the contour until reaching the destination point (B) near the bottom of a canyon. The cumulative travel times associated with traveling along this route can be seen in Fig. 11. The modeled median (50th percentile) travel time for traversing this path is 93 min; however, the percentile models can be used to predict time ranges for various portions of the population. For example, using the 2.5th and 97.5th percentile models, we estimate that 95% of the population would hike from A to B between 66 and 141 min. To estimate the range of times for a known faster population (e.g., a wildland fire crew or military personnel), a narrower and higher range of percentiles can be used, such as the 50th and 97.5th, though the specific selection of subpopulation percentiles should be independently validated.

4. Discussion

Our research provides valuable insight into the complex process of estimating variability in travel rates and times. Humans are inherently variable in many ways that directly affect their pedestrian behaviors, such as height, weight, stride length, fitness level, endurance level, energy expenditure, load carriage, familiarity and comfort level with diverse terrain, and more. By gathering GPS data from over 2000 individuals, and using trails of different lengths, at different elevations, and different levels of difficulty, the percentile travel rate functions we developed using this dataset are intended to be representative of a broad population of hikers within the US. However, these travel rate functions may not be inclusive of all hikers due to inherent limitations in the dataset. First, we do not have any demographic information about the study's sample population, as AllTrails profiles did not provide gender, age, or other potentially insightful individual characteristics at the time of data acquisition. Thus, we do not know the extent to which our population is demographically representative of the US population as a whole and were unable to use those demographics to understand potential drivers of travel rate variability. For example, the data that were used to develop the predictive functions came from trails near large urban centers, which may suggest that the median age of our sample population is younger than those in more rural settings. Enthusiasts may be more likely to record their GPS tracks, and people with disabilities may be underrepresented in the dataset. The bias towards such enthusiasts in our dataset may results in a flatter slope-travel rate curve, given the fact that fit individuals are likely to be less affected by terrain slope. Also, hikers may "self-select" trail difficulty (including length and slope) based on their abilities. This can act to provide an upward bias in overall travel rates, as inexperienced or unfit hikers may avoid more challenging trails with steeper slopes, the exclusion of which could potentially reduce the number of low-speed data points. Although it may be possible in the future to incorporate additional intrinsic and extrinsic factors into a singular, all-encompassing predictive model, there are currently no such datasets that can allow for this. In lieu of such a model, we have presented a robust set of percentile-based travel rate predictive models that can be applied directly to the important problem of predicting ranges of travel times within a margin of error of approximately ±9%.

Data from this study were gleaned from hikes that took place on trails. We do not know the exact surface types or conditions of the trails studied, but they may range from dirt to gravel, loose to packed, wet to dry, and smooth to rough. In many of the aforementioned applications

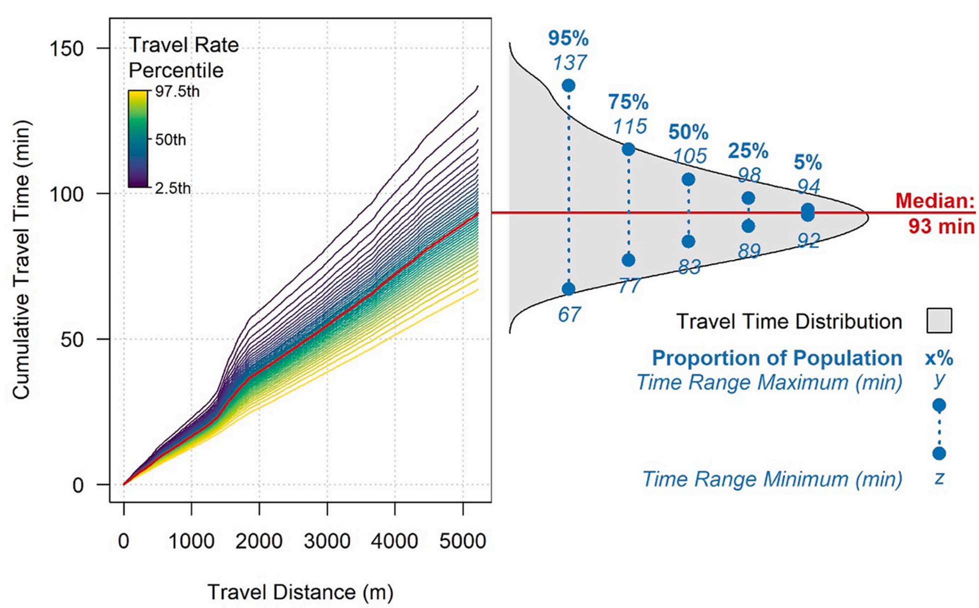

Fig. 11. Cumulative travel times and the associated distribution thereof, as illustrated by a kernel density estimator, for a simulated population hiking along the least-cost path in Fig. 10.

for travel time prediction – particularly those that take place in urban settings – pedestrian travel will likely be on paved surfaces (roads and sidewalks). Although roads and trails are similar, studies have shown that traversing gravel/dirt surfaces requires slightly higher energy expenditure (Pandolf et al., 1977; Richmond, Potter, & Santee, 2015). Thus, at the same level of energy expenditure, we can assume that movement on a trail is slightly slower than that of a paved road. It is quite common to apply predictive functions derived from trail hiking data to the prediction of travel rates and times in urban settings (e.g., Wood & Schmidtlein, 2012). Thus, we suggest that the results of our study can be applied to travel on road networks with the understanding that travel times might be overestimated.

In this study, we removed stoppage time from the GPS data and did not consider it in our travel rate and travel time analyses. We opted to take this approach as it would be difficult to predict how long individuals would rest while on a hike, with some perhaps taking only brief respites while others may stop for lengthy periods of time (e.g., resting after reaching a mountain summit). This has two important implications. First, applying the travel rate predictive functions we have presented to estimate total travel times will only capture continuous movement time. Assuming that the typical hiker or walker will take at least one break during an activity, this means that our predictions will generally underestimate the total, stoppage-inclusive travel time. Second, resting while on a hike can provide a necessary energetic recharge to an individual (e.g., temporarily lowering one's heart rate). This could increase the level of energy one could exert while in motion between breaks, as compared to trying to maintain a lower, but more sustainable level of exertion for continuous movement.

Least-cost path modeling is one of the most common analysis techniques that relies on robust equations for predicting the rate of travel, given a set of landscape impediments. In this study, we presented one such example, using our newly-generated predictive functions for both mapping the least-cost path and estimating the ranges of likely travel times to traverse the path. However, it is important to note the limitations of applying a function that was derived from on-trail travel in an off-trail environment, particularly with respect to the impact of vegetation cover on travel rate, travel time, and optimal route selection (Campbell et al., 2017; Richmond et al., 2015). Off-trail travel may also involve uncompacted, rough, or otherwise difficult to traverse surfaces, which can significantly affect travel rates (Campbell et al., 2017; Irmischer & Clarke, 2018; Richmond et al., 2015). Future work should aim to refine our understanding of the effects of vegetation structure and ground surface conditions on travel rates.

Although we produced 39 separate percentile-based predictive models, and the full consideration of all of those models enables the prediction of travel time distributions, not every user will be interested in making 39 separate predictions. We would encourage those with an interest in predicting travel times using our models to focus on three models. The first should be the 50th percentile travel rate function. This represents the slope-controlled travel rate of an average hiker, and thus is the most broadly-applicable among our functions. The selection of the other two depends on the user's needs. For example, the 2.5th and 97.5th travel rate functions produce times representing the range within which 95% of the population will arrive at a destination, given an origin location. Other percentile ranges may be more appropriate for specific populations. For example, for a population that moves faster than average hikers (e.g., wildland firefighters), a higher range of percentile functions may be selected.

5. Conclusions

In this study, we have presented a new approach for estimating the variability in pedestrian travel rates and times, driven by the slope of the terrain, using a database containing over 5 million GPS-tracked travel rate records, a significant increase over the next largest study's sample size (Campbell, Dennison, et al., 2019). Previous pedestrian travel rate literature has been limited by either (a) being tailored to the individual, which limits the capacity for estimation at the population level; or (b) resulting in oversimplified, population-level predictive functions, which lack the capacity to estimate variability in travel rates and times. The work we have presented offers robust, independently-validated equations for predicting travel rates and times that can be used in a variety of applications. The median model, representing the travel rate of a typical hiker, demonstrated improvement over previous slope-travel rate functions, with a 9% improvement in RMSE and 87% improvement in bias as compared to the next-best model. This model likewise demonstrated improvement in the prediction of travel times over existing functions, with an absolute bias of only 2 min averaged across three independent test trails. The full range of percentile models was able to estimate travel time ranges within a margin of error of approximately 9% of total travel time. In the presence of trails and/or roads, these equations can be used in conjunction with a digital elevation model for estimating along-network travel times and selecting optimal travel routes within a network. In the absence of such a transportation network, these equations can be applied using least-cost path modeling. However, both of these endeavors should be undertaken cautiously, as vegetation and ground surface conditions are not considered in the results of this study.

Disclaimer

The findings and conclusions in this report are those of the authors and should not be construed to represent any official USDA or U.S. Government determination or policy. Any use of trade, firm, or product names is for descriptive purposes only and does not imply endorsement by the U.S. government.

Funding

This work was supported by the National Science Foundation (#BCS-2117865) and the USDA Forest Service (#21-CS-11221636-120).

CRediT authorship contribution statement

Michael J. Campbell: Conceptualization, Methodology, Software, Validation, Formal analysis, Investigation, Data curation, Writing – original draft, Writing – review & editing, Visualization, Supervision, Project administration, Funding acquisition. **Philip E. Dennison:** Conceptualization, Methodology, Writing – original draft, Writing – review & editing, Supervision, Funding acquisition. **Matthew P. Thompson:** Methodology, Writing – original draft, Supervision, Funding acquisition.

Declaration of Competing Interest

None.

Appendix

Table A1
Summary of GPS track data.

State	Trail Name	Length (m)	N_{tracks}	N_{people}	$N_{points, pre-filter}$	$N_{points, post-filter}$
CA	Black Star Canyon Falls Trail	10,662	45	45	117,956	79,863
CA	Bridge To Nowhere Via East Fork Trail	15,214	119	118	405,604	316,111
CA	Eaton Canyon Trail	6848	137	136	190,207	136,878
CA	Echo Mountain Via Sam Merrill Trail	8063	115	94	240,034	175,422
CA	Icehouse Canyon to Cucamonga Peak Trail	17,882	95	95	442,768	354,261
CA	Mount San Antonio and Mount Baldy Notch Trail	15,634	142	140	552,560	422,176
CA	Runyon Canyon Trail	4198	75	72	73,311	51,619
CA	Solstice Canyon Loop	4699	121	121	149,680	114,908
CA	Switzer Falls Via Gabrielino Trail	5715	63	63	91,502	68,725
CA	Temescal Canyon Trail	5885	110	107	132,395	99,476
UT	Bells Canyon Trail to Lower Falls	7296	110	108	191,358	148,680
UT	Cecret Lake Trail	2824	74	74	51,802	42,218
UT	Donut Falls Trail	5231	84	84	72,535	52,591
UT	Gloria Falls	3423	164	164	140,598	109,920
UT	Grandeur Peak East Trail from Church Fork	8716	34	33	75,415	59,478
UT	Lake Blanche Trail	12,453	199	196	539,960	436,600
UT	Lake Mary Trail	4219	99	98	94,292	77,005
UT	Living Room Lookout Trail	3706	44	43	38,216	30,729
UT	Mount Olympus Trail	10,309	58	55	162,335	109,492
UT	Red Pine Lake Trail	10,978	111	109	294,663	221,730
	Total	**163,955**	**1999**	**1955**	**4,057,191**	**3,107,882**

Table A2
GPS track data used for testing travel time variability predictions.

State	Trail Name	Length (m)	N_{tracks}	N_{people}	$N_{points, pre-filter}$	$N_{points, post-filter}$
NH	Mount Willard Trail	4734	104	103	136,232	131,932
TN	Alum Cave Trail to Mount LeConte	15,446	121	119	470,664	453,822
WA	Skyline Trail Loop	8198	245	244	555,722	530,592
	Total	**28,378**	**470**	**466**	**1,162,618**	**1,116,346**

Table A3
Model coefficients for percentile models derived from non-linear quantile regression.

Percentile	a	b	c	d	e
2.5	−1.4190	19.1535	54.2746	−0.0215	7.9526×10^{-4}
5.0	−1.3914	20.2136	61.6700	−0.0459	9.2172×10^{-4}
7.5	−1.4515	20.9310	65.8647	−0.0516	8.1817×10^{-4}
10.0	−1.4921	20.8687	65.9137	−0.0329	6.7077×10^{-4}
12.5	−1.5744	20.5100	64.2547	−0.0034	6.2977×10^{-4}
15.0	−1.6177	20.4735	64.5461	0.0075	5.7225×10^{-4}
17.5	−1.6107	19.9227	62.1549	0.0378	4.7355×10^{-4}
20.0	−1.6236	19.8539	62.1986	0.0480	4.4430×10^{-4}
22.5	−1.6396	19.3788	60.0472	0.0762	4.1543×10^{-4}
25.0	−1.6920	19.4639	60.8517	0.0799	4.2500×10^{-4}
27.5	−1.7100	19.4143	60.8487	0.0902	3.8552×10^{-4}
30.0	−1.7148	19.2929	60.4638	0.1032	3.3948×10^{-4}
32.5	−1.7245	20.0529	64.6180	0.0793	3.3463×10^{-4}
35.0	−1.6867	20.2394	65.6540	0.0804	2.4034×10^{-4}
37.5	−1.6601	20.1343	65.2359	0.0922	1.5992×10^{-4}
40.0	−1.6161	20.0784	65.0172	0.1027	5.2507×10^{-5}
42.5	−1.6074	21.0144	70.2841	0.0706	1.1865×10^{-5}
45.0	−1.5730	21.6438	74.0125	0.0513	-7.1719×10^{-5}
47.5	−1.5227	21.9340	75.6591	0.0480	-1.8281×10^{-4}
50.0	−1.4579	22.0787	76.3271	0.0525	-3.2002×10^{-4}
52.5	−1.4254	21.9986	75.6166	0.0675	-3.9490×10^{-4}
55.0	−1.3802	22.4770	78.2737	0.0583	-5.1117×10^{-4}
57.5	−1.3416	23.2824	83.1265	0.0338	-6.1657×10^{-4}
60.0	−1.3138	23.8222	86.2342	0.0232	-6.8611×10^{-4}
62.5	−1.3025	23.9738	86.6684	0.0322	-7.5286×10^{-4}
65.0	−1.3137	23.6565	83.8119	0.0650	-7.8491×10^{-4}
67.5	−1.3157	23.8571	84.2605	0.0756	-8.4548×10^{-4}
70.0	−1.2750	24.2517	85.7576	0.0803	-9.7634×10^{-4}
72.5	−1.2710	23.9933	82.7877	0.1173	-1.0212×10^{-3}
75.0	−1.2842	23.1097	75.7319	0.1852	-1.0541×10^{-3}

(continued on next page)

Table A3 (*continued*)

Percentile	a	b	c	d	e
77.5	−1.2464	23.4466	76.0881	0.2019	-1.1644×10^{-3}
80.0	−1.1997	23.0571	71.9543	0.2524	-1.3087×10^{-3}
82.5	−1.1673	21.7316	62.7781	0.3429	-1.4094×10^{-3}
85.0	−1.1299	21.7936	60.8815	0.3825	-1.5038×10^{-3}
87.5	−1.2537	20.6660	52.7387	0.4759	-1.3440×10^{-3}
90.0	−1.4109	19.8424	46.8318	0.5561	-1.1847×10^{-3}
92.5	−1.5847	18.2614	38.5108	0.6645	-1.1161×10^{-3}
95.0	−1.7612	16.4733	31.5181	0.7733	-1.0611×10^{-3}
97.5	−2.0921	16.8711	31.2808	0.8493	-8.3866×10^{-4}

References

Adriaensen, F., Chardon, J. P., De Blust, G., Swinnen, E., Villalba, S., Gulinck, H., & Matthysen, E. (2003). The application of 'least-cost' modelling as a functional landscape model. *Landscape and Urban Planning, 64*(4), 233–247. https://doi.org/10.1016/S0169-2046(02)00242-6

dos Anjos Luis, A., & Cabral, P. (2016). Geographic accessibility to primary healthcare centers in Mozambique. *International Journal for Equity in Health, 15*(1), 173. https://doi.org/10.1186/s12939-016-0455-0

Beighley, M. (1995). Beyond the safety zone: Creating a margin of safety. *Fire Management Notes, 55*(4), 21–24.

Bernardini, G., Santarelli, S., Quagliarini, E., & D'Orazio, M. (2017). Dynamic guidance tool for a safer earthquake pedestrian evacuation in urban systems. *Computers, Environment and Urban Systems, 65*, 150–161. https://doi.org/10.1016/j.compenvurbsys.2017.07.001

Campbell, M. J., Dennison, P. E., & Butler, B. W. (2017). A LiDAR-based analysis of the effects of slope, vegetation density, and ground surface roughness on travel rates for wildland firefighter escape route mapping. *International Journal of Wildland Fire, 26*(10), 884–895. https://doi.org/10.1071/WF17031

Campbell, M. J., Dennison, P. E., Butler, B. W., & Page, W. G. (2019). Using crowdsourced fitness tracker data to model the relationship between slope and travel rates. *Applied Geography, 106*, 93–107. https://doi.org/10.1016/j.apgeog.2019.03.008

Campbell, M. J., Page, W. G., Dennison, P. E., & Butler, B. W. (2019). Escape route index: A spatially-explicit measure of wildland firefighter egress capacity. *Fire, 2*(3), 40. https://doi.org/10.3390/fire2030040

Carver, S., Comber, A., McMorran, R., & Nutter, S. (2012). A GIS model for mapping spatial patterns and distribution of wild land in Scotland. *Landscape and Urban Planning, 104*(3), 395–409. https://doi.org/10.1016/j.landurbplan.2011.11.016

Chen, B. Y., Wang, Y., Wang, D., & Lam, W. H. K. (2019). Understanding travel time uncertainty impacts on the equity of individual accessibility. *Transportation Research Part D: Transport and Environment, 75*, 156–169. https://doi.org/10.1016/j.trd.2019.08.027

Chen, B. Y., Yuan, H., Li, Q., Wang, D., Shaw, S.-L., Chen, H.-P., & Lam, W. H. K. (2017). Measuring place-based accessibility under travel time uncertainty. *International Journal of Geographical Information Science, 31*(4), 783–804. https://doi.org/10.1080/13658816.2016.1238919

Chen, C., Mostafizi, A., Wang, H., Cox, D., & Cramer, L. (2022). Evacuation behaviors in tsunami drills. *Natural Hazards*. https://doi.org/10.1007/s11069-022-05208-y

Chiou, C.-R., Tsai, W.-L., & Leung, Y.-F. (2010). A GIS-dynamic segmentation approach to planning travel routes on forest trail networks in Central Taiwan. *Landscape and Urban Planning, 97*(4), 221–228. https://doi.org/10.1016/j.landurbplan.2010.06.004

Ciesa, M., Grigolato, S., & Cavalli, R. (2014). Analysis on vehicle and walking speeds of search and rescue ground crews in mountainous areas. *Journal of Outdoor Recreation and Tourism, 5–6*, 48–57. https://doi.org/10.1016/j.jort.2014.03.004

Davey, R. C., Hayes, M., & Norman, J. M. (1994). Running uphill: An experimental result and its applications. *The Journal of the Operational Research Society, 45*(1), 25–29. https://doi.org/10.2307/2583947

Doherty, P. J., Guo, Q., Doke, J., & Ferguson, D. (2014). An analysis of probability of area techniques for missing persons in Yosemite National Park. *Applied Geography, 47*, 99–110. https://doi.org/10.1016/j.apgeog.2013.11.001

Douglas, D. H. (1994). Least-cost path in GIS using an accumulated cost surface and slopelines. *Cartographica: The International Journal for Geographic Information and Geovisualization, 31*(3), 37–51. https://doi.org/10.3138/D327-0323-2JUT-016M

Ettema, D., & Timmermans, H. (2006). Costs of travel time uncertainty and benefits of travel time information: Conceptual model and numerical examples. *Transportation Research Part C: Emerging Technologies, 14*(5), 335–350. https://doi.org/10.1016/j.trc.2006.09.001

Ewing, R., & Handy, S. (2009). Measuring the unmeasurable: Urban design qualities related to walkability. *Journal of Urban Design, 14*(1), 65–84. https://doi.org/10.1080/13574800802451155

Fields, M. A. (1995). *Preliminary Applications of the Variable Resolution Terrain Model to a Troop Movement Model*. Army Research Lab Aberdeen Proving Ground MD. https://apps.dtic.mil/sti/citations/ADA299315.

Fraser, S. A., Wood, N. J., Johnston, D. M., Leonard, G. S., Greening, P. D., & Rossetto, T. (2014). Variable population exposure and distributed travel speeds in least-cost tsunami evacuation modelling. *Natural Hazards and Earth System Sciences Discussions, 2*, 4163–4200. https://doi.org/10.5194/nhessd-2-4163-2014

Goodchild, M. F. (1977). An evaluation of lattice solutions to the problem of corridor location. *Environment and Planning A, 9*(7), 727–738. https://doi.org/10.1068/a090727

Goodchild, M. F. (2020). Beyond Tobler's hiking function. *Geographical Analysis, 52*(4), 558–569. https://doi.org/10.1111/gean.12253

Gottschall, J. S., & Kram, R. (2003). Energy cost and muscular activity required for propulsion during walking. *Journal of Applied Physiology, 94*(5), 1766–1772. https://doi.org/10.1152/japplphysiol.00670.2002

Herzog, I. (2010). *Theory and practice of cost functions*. In (pp. 375–382).

Herzog, I. (2014). Least-cost paths–some methodological issues. *Internet Archaeology, 36* (10.11141).

Higgins, C. D. (2021). Hiking with Tobler: Tracking movement and calibrating a cost function for personalized 3D accessibility. *Findings, 28107*. https://doi.org/10.32866/001c.28107

Irmischer, I. J., & Clarke, K. C. (2018). Measuring and modeling the speed of human navigation. *Cartography and Geographic Information Science, 45*(2), 177–186. https://doi.org/10.1080/15230406.2017.1292150

Kay, A. (2012). Pace and critical gradient for hill runners: An analysis of race records. *Journal of Quantitative Analysis in Sports, 8*(4). https://doi.org/10.1515/1559-0410.1456

Kliskey, A. D. (2000). Recreation terrain suitability mapping: A spatially explicit methodology for determining recreation potential for resource use assessment. *Landscape and Urban Planning, 52*(1), 33–43. https://doi.org/10.1016/S0169-2046(00)00111-0

Korpilo, S., Virtanen, T., & Lehvävirta, S. (2017). Smartphone GPS tracking—Inexpensive and efficient data collection on recreational movement. *Landscape and Urban Planning, 157*, 608–617. https://doi.org/10.1016/j.landurbplan.2016.08.005

Looney, D. P., Santee, W. R., Hansen, E. O., Bonventre, P. J., Chalmers, C. R., & Potter, A. W. (2019). Estimating energy expenditure during level, uphill, and downhill walking. *Medicine and Science in Sports and Exercise, 51*(9), 1954–1960. https://doi.org/10.1249/MSS.0000000000002002

Ludlow, L. W., & Weyand, P. G. (2017). Walking economy is predictably determined by speed, grade, and gravitational load. *Journal of Applied Physiology, 123*(5), 1288–1302. https://doi.org/10.1152/japplphysiol.00504.2017

Márquez-Pérez, J., Vallejo-Villalta, I., & Álvarez-Francoso, J. I. (2017). Estimated travel time for walking trails in natural areas. *Geografisk Tidsskrift-Danish Journal of Geography, 117*(1), 53–62. https://doi.org/10.1080/00167223.2017.1316212

Meijles, E. W., de Bakker, M., Groote, P. D., & Barske, R. (2014). Analysing hiker movement patterns using GPS data: Implications for park management. *Computers, Environment and Urban Systems, 47*, 44–57. https://doi.org/10.1016/j.compenvurbsys.2013.07.005

Merry, K., & Bettinger, P. (2019). Smartphone GPS accuracy study in an urban environment. *PLoS One, 14*(7), Article e0219890. https://doi.org/10.1371/journal.pone.0219890

Minetti, A. E., Moia, C., Roi, G. S., Susta, D., & Ferretti, G. (2002). Energy cost of walking and running at extreme uphill and downhill slopes. *Journal of Applied Physiology, 93*(3), 1039–1046. https://doi.org/10.1152/japplphysiol.01177.2001

Naismith, W. (1892). Cruach Adran, Stobinian, and Ben More. *Scottish Mountaineering Club Journal, 2*(3), 136.

Orsi, F., & Geneletti, D. (2016). Transportation as a protected area management tool: An agent-based model to assess the effect of travel mode choices on hiker movements. *Computers, Environment and Urban Systems, 60*, 12–22. https://doi.org/10.1016/j.compenvurbsys.2016.07.008

de Palma, A., & Picard, N. (2005). Route choice decision under travel time uncertainty. *Transportation Research Part A: Policy and Practice, 39*(4), 295–324. https://doi.org/10.1016/j.tra.2004.10.001

Pandolf, K. B., Givoni, B., & Goldman, R. F. (1977). Predicting energy expenditure with loads while standing or walking very slowly. *Journal of Applied Physiology: Respiratory, Environmental and Exercise Physiology, 43*(4), 577–581.

Peterson, B. A., Brownlee, M. T. J., & Marion, J. L. (2018). Mapping the relationships between trail conditions and experiential elements of long-distance hiking. *Landscape and Urban Planning, 180*, 60–75. https://doi.org/10.1016/j.landurbplan.2018.06.010

Rees, W. G. (2004). Least-cost paths in mountainous terrain. *Computers & Geosciences, 30*(3), 203–209. https://doi.org/10.1016/j.cageo.2003.11.001

Reyes, M., Páez, A., & Morency, C. (2014). Walking accessibility to urban parks by children: A case study of Montreal. *Landscape and Urban Planning, 125*, 38–47. https://doi.org/10.1016/j.landurbplan.2014.02.002

Richmond, P. W., Potter, A. W., & Santee, W. R. (2015). Terrain factors for predicting walking and load carriage energy costs: Review and refinement. *Journal of Sport and Human Performance, 3*(3). https://doi.org/10.12922/jshp.v3i3.67

Rout, A., Nitoslawski, S., Ladle, A., & Galpern, P. (2021). Using smartphone-GPS data to understand pedestrian-scale behavior in urban settings: A review of themes and approaches. *Computers, Environment and Urban Systems, 90*, Article 101705. https://doi.org/10.1016/j.compenvurbsys.2021.101705

Rustamov, R. B., & Hashimov, A. M. (2018). *Multifunctional operation and application of GPS*. BoD – Books on Demand.

Santee, W. R., Blanchard, L. A., Speckman, K. L., Gonzalez, J. A., & Wallace, R. F. (2003). *Load Carriage Model Development and Testing with Field Data*. Army Research Inst Of Environmental Medicine Natick MA. https://apps.dtic.mil/sti/citations/ADA415788.

Santerre, R., Geiger, A., & Banville, S. (2017). Geometry of GPS dilution of precision: Revisited. *GPS Solutions, 21*(4), 1747–1763.

Shalev, K., Schaefer, M., & Morgan, A. (2009). Investigating missing person cases: How can we learn where they go or how far they travel? *International Journal of Police Science and Management, 11*(2), 123–129. https://doi.org/10.1350/ijps.2009.11.2.116

Sugarbaker, L. J., Eldridge, D. F., Jason, A. L., Lukas, V., Saghy, D. L., Stoker, J. M., & Thunen, D. R. (2017). *Status of the 3D Elevation Program, 2015 (USGS Numbered Series No. 2016–1196; Open-File Report)*. U.S. Geological Survey. http://pubs.er.usgs.gov/publication/ofr20161196.

Sullivan, P. R., Campbell, M. J., Dennison, P. E., Brewer, S. C., & Butler, B. W. (2020). Modeling wildland firefighter travel rates by terrain slope: Results from GPS-tracking of type 1 crew movement. *Fire, 3*(3), 52. https://doi.org/10.3390/fire3030052

Tobler, W. (1993). *Three presentations on geographical analysis and modeling. No. 93–1* p. 24). National Center for Geographic Information and Analysis.

White, D. A. (2015). The basics of least cost analysis for archaeological applications. *Advances in Archaeological Practice, 3*(4), 407–414. https://doi.org/10.7183/2326-3768.3.4.407

Widener, M. J., Minaker, L., Farber, S., Allen, J., Vitali, B., Coleman, P. C., & Cook, B. (2017). How do changes in the daily food and transportation environments affect grocery store accessibility? *Applied Geography, 83*, 46–62. https://doi.org/10.1016/j.apgeog.2017.03.018

Wolf, I. D., & Wohlfart, T. (2014). Walking, hiking and running in parks: A multidisciplinary assessment of health and well-being benefits. *Landscape and Urban Planning, 130*, 89–103. https://doi.org/10.1016/j.landurbplan.2014.06.006

Wood, N. J., & Schmidtlein, M. C. (2012). Anisotropic path modeling to assess pedestrian-evacuation potential from Cascadia-related tsunamis in the US Pacific Northwest. *Natural Hazards, 62*(2), 275–300. https://doi.org/10.1007/s11069-011-9994-2

Wu, T., & Zhao, Y. (2021). Associations between functional fitness and walking speed in older adults. *Geriatric Nursing, 42*(2), 540–543. https://doi.org/10.1016/j.gerinurse.2020.10.003

Xiang, W.-N. (1996). A GIS based method for trail alignment planning. *Landscape and Urban Planning, 35*(1), 11–23. https://doi.org/10.1016/0169-2046(96)00303-9

Yang, Y., Auchincloss, A. H., Rodriguez, D. A., Brown, D. G., Riolo, R., & Diez-Roux, A. V. (2015). Modeling spatial segregation and travel cost influences on utilitarian walking: Towards policy intervention. *Computers, Environment and Urban Systems, 51*, 59–69. https://doi.org/10.1016/j.compenvurbsys.2015.01.007